Quantitative imaging of mixing dynamics in microfluidic droplets using two-photon fluorescence lifetime imaging

Yan Zeng,[1,†] Liguo Jiang,[2,†] Wei Zheng,[1] Dong Li,[1] Shuhuai Yao,[2,3,4] and Jianan Y. Qu[1,2,*]

[1]*Department of Electronic and Computer Engineering, Hong Kong University of Science and Technology, Hong Kong, China*

[2]*Bioengineering Graduate Program, Hong Kong University of Science and Technology, Hong Kong, China*

[3]*Department of Mechanical Engineering, Hong Kong University of Science and Technology, Hong Kong, China*

[4]*e-mail: meshyao@ust.hk*

**Corresponding author: eequ@ust.hk*

Received March 9, 2011; revised May 6, 2011; accepted May 11, 2011;
posted May 13, 2011 (Doc. ID 143893); published June 7, 2011

Droplet-based microfluidic systems enable miniaturization of chemical reactions in femtoliter to picoliter volume compartments. Quantifying mixing dynamics of the reagents in droplets is critical to determine the system performance. In this Letter, we developed a two-photon excitation fluorescence lifetime imaging technique to quantitatively image the mixing dynamics in microfluidic droplets. A cross/autocorrelation method was used to reconstruct a high-quality fluorescence lifetime image of the droplet. The fluorescence decay was analyzed for accurate determination of the mixing ratio at each pixel of the image. © 2011 Optical Society of America

OCIS codes: 110.3010, 180.4315, 190.4180.

Droplet-based microfluidic systems have recently emerged as a new and exciting technological platform for a variety of applications, including synthesis of micro/nanoparticles, protein crystallization, enzyme kinetic studies, and DNA amplification [1,2]. The generated high-throughput droplets, with unique features, such as no reagent dispersion, rapid mixing, high controllability, and high reproducibility, can be treated as "artificial cells" or "isolated microreactors" for fast reactions after the mixing of reagents. It has been reported that protein crystallization, as well as the yields and size distributions of the synthesized nanoparticles, was significantly affected by the mixing dynamics within droplets [3,4]. Therefore, a quantitative method to measure the mixing dynamics in droplets is indispensible for understanding the physics of mixing in droplets and for characterization of the droplet-based microfluidic system.

The conventional method to study mixing patterns is based on a standard microscope with a CCD camera [1–4]. The drawback is that the image captured by the CCD is the projection of a 3D droplet to a 2D image plane. A laser scanning fluorescence lifetime microscope (FLIM) was employed to provide a robust means for imaging the mixing in the continuous laminar flow of a microfluidic device [5]. This method cannot be directly applied to image the droplet mixing due to the discrete nature of droplet generation. Recently, confocal FLIM based on the maximum likelihood estimator (MLE) method was used to analyze the fluorescence lifetime images of microfluidic droplets [6,7]. Using a small number of photons, the MLE method can determine the fluorescence lifetime with large error. In this study, we build a line-scanning two-photon FLIM for the quantitative imaging of dynamic mixing in droplets. The line scanning along the microfluidic channel is passively achieved via the droplets flowing through the excitation focal point. Because the periodically generated droplets are identical, we scan multiple droplets and sum up the line signals of each droplet to obtain the line signal with a high signal-to-noise ratio. The droplets are scanned line by line by moving the focal point across the channel using a translation stage. The cross-sectional image of the droplet is then formed by aligning the scanning lines across the channel. Two commercial fluorescence dyes (Lucifer Yellow and Alexa 430, Invitrogen) with similar absorption/emission spectra and different fluorescence lifetimes are used as the indicators of two mixing fluids. A nonfitting method is developed to accurately calculate the mixing ratios.

The droplet-based microfluidic system used in this study (shown in Fig. 1) is a flow-focusing microchannel with a cross section of $50\,\mu\text{m} \times 50\,\mu\text{m}$. The device was fabricated with polydimethylsiloxane utilizing a standard soft lithography process [7]. Alexa 430 and Lucifer Yellow solutions were pumped into the central inlet and the two side inlets at flow rates of $1\,\mu$liter/ min and $0.5\,\mu$liter/ min, respectively. The solutions flowed into the junction in parallel and were intersected with two mineral oil streams from two side channels at a flow rate of $1.25\,\mu$liter/ min. The mixing dynamics of two solutions was studied experimentally using a homemade two-photon FLIM, modified from the previously reported FLIM system [8]. Briefly, a tunable femtosecond Ti:sapphire laser (850 nm) was employed as the excitation source. A water immersion objective lens (60×, 1.20 NA, Olympus) was used to focus the laser into the microchannel that was mounted on a precision translation stage (V-102, Physik Instrument). The focal point was set at $25\,\mu$m height, half of the channel depth, and scanned across the channel at a $1\,\mu$m interval. The backscattered fluorescence signal and excitation were

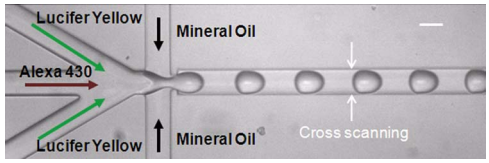

Fig. 1. (Color online) Image of droplet generation captured by a CCD camera. The scale bar is $50\,\mu$m.

separated by a dichroic mirror (735 nm, Semrock). The fluorescence signal was detected by a photomultiplier tube (PMT). A short pass filter (740 nm, Chroma) and a bandpass filter (550 ± 20 nm, Thorlabs) were placed in front of the PMT to reject the residual reflection and Rayleigh scattering of the excitation light. The intensity and lifetime of the two-photon fluorescence signals were recorded by a time-correlated single-photon counting (TCSPC) system (SPC-150, Becker & Hickl GmbH).

The raw data of fluorescence decay measured from two fluorescence dyes are shown in Fig. 2(a). The decay curves were well fit in the single exponential form after deconvolution from the system response. The results showed that the lifetime of Lucifer fluorescence is about 2 ns longer than Alexa 430, indicating that two fluorescence signals could be well separated in the time domain. To make use of the fluorescence dyes as the quantitative indicators of two different flows, we measured the time-resolved fluorescence signals from 11 solutions with mixing ratios of Lucifer and Alexa 430 dyes ranged from 0%–100% with a 10% interval. The mixing ratios for the dye solutions were defined as $M_{\text{Alexa}} = C_{N\text{-Alexa}}/(C_{N\text{-Alexa}} + C_{N\text{-Lucifer}})$ and $M_{\text{Lucifer}} = (1 - M_{\text{Alexa}})$, where $C_{N\text{-Alexa}}$ and $C_{N\text{-Lucifer}}$ were the normalized concentrations, the ratios of the dye concentrations in the mixing solutions over those in the pure solutions ($C_{N\text{-Alexa}} = C_{\text{Alexa}}/C_{P\text{-Alexa}}$, and $(C_{N\text{-Lucifer}} = C_{\text{Lucifer}}/C_{P\text{-Lucifer}})$, respectively [9].

We first used the conventional least-squares (LS) fitting approach to calculate the mixing ratios. The measured fluorescence decay signals were fitted using a dual exponential fitting model. Two fitting parameters, the amplitudes of two exponential decay terms, A_{Alexa} and A_{Lucifer}, were obtained from the LS fitting and could be directly used to calculate the mixing ratios, $M_{\text{Alexa}} = (A_{\text{Alexa}}/A_{\text{Alexa-pure}})/(A_{\text{Alexa}}/A_{\text{Alexa-pure}} + A_{\text{Lucifer}}/A_{\text{Lucifer-pure}})$ where $A_{\text{Alexa-pure}}$ and $A_{\text{Lucifer-pure}}$ were the amplitudes of the fluorescence decay terms measured from pure Alexa and Lucifer solutions, respectively. We found that a large number of photon counts were required to achieve high accuracy in the LS fitting [10]. As shown in Fig. 2(b), the fitting errors increased rapidly with the decrease of the photon counts ($<2 \times 10^5$). This makes the LS fitting method impractical when a measurement cannot produce sufficient photon counts [7]. In this study, we developed a simple nonfitting method based on the ratio of fluorescence signals in two decay regions, the peak region and the tail region, as shown in Fig. 2(a). The concept of the division method is to produce a calibration curve based on the experimentally measured division ratio (D_{Ratio}) of the photon counts in the peak region (I_{Peak}) over the tail (I_{Tail}) region:

$$D_{\text{Ratio}} = \frac{I_{\text{Peak}}}{I_{\text{Tail}}} = \frac{M_{\text{Alexa}} \times I_{P-\text{Alexa}} + (1 - M_{\text{Alexa}}) \times I_{P-\text{Lucifer}}}{M_{\text{Alexa}} \times I_{T-\text{Alexa}} + (1 - M_{\text{Alexa}}) \times I_{T-\text{Lucifer}}}, \quad (1)$$

where I_P and I_T are the photon counts in the peak and tail regions measured from pure Alexa and Lucifer solutions under the same condition, respectively. The peak and tail time window widths were set to be identical. The mixing ratios, M_{Alexa} and M_{Lucifer}, then can be calculated from Eq. (1) based on the experimentally measured division ratio, D_{Ratio}. The division ratios measured from 11 mixing solutions are shown in Fig. 2(c) (triangles). As a comparison, the mixing ratios calculated from Eq. (1) with M_{Alexa} values varying from 0%–100% are also presented in Fig. 2(c) (green curve). The results demonstrate excellent agreement between the calculation and experimental measurements, indicating that the green curve in Fig. 2(c) can be used as a calibration to find a mixing ratio corresponding to a measured division ratio. We found that about 1% standard error of the reconstructed mixing ratio was achieved at 2×10^5 photon counts. More importantly, the mixing ratios could be recovered accurately even at the photon count level as low as 1000, as shown in Fig. 2(d). The simple division method requires a much smaller number of photon counts to achieve high accuracy in the calculation of mixing ratios of Alexa and Lucifer solutions. The improvement over the LS fitting method is due to the significantly increased SNR by using the summed counts in two time windows for the analysis.

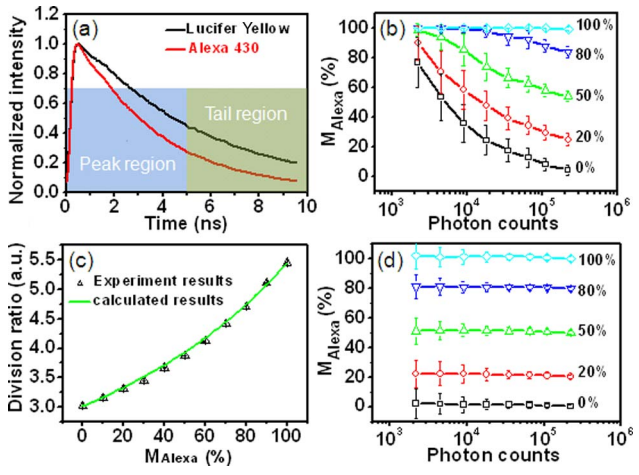

Fig. 2. (Color online) Fluorescence characteristics of two mixing solutions. (a) Fluorescence decays for Lucifer (lifetime~ 5.0 ns) and Alexa 430 (lifetime ~ 3.1 ns). (b) Calculated mixing ratio as a function of photon counts using the LS approach. (c) Measured and calculated mixing ratios from 11 bulk solutions using the division ratio method. (d) Calculated mixing ratio as a function of photon counts using the division ratio method.

Next, we conducted fluorescence imaging of the droplet-based microfluidic device using our two-photon excitation FLIM system. Before the fluorescence measurement, a CCD camera was used to confirm the stable generation of droplets. The wide-field image in Fig. 1 shows the droplets, separated by the immiscible mineral oil. The generation rate of droplets was about 500/s, corresponding to 60 mm/s in velocity. A representative signal of line scanning over five droplets is shown in Fig. 3(a). As can be seen, the photon counts for each droplet were obviously low (maximal counts ~25) due to the high droplet generation rate and low excitation level. To improve the quality of the line-scanning signal for accurate mapping of the mixing ratios within the droplets, we summed up the signals measured from multiple droplets to increase the photon counts at each pixel of the droplet image. Because of the limitation of data storage

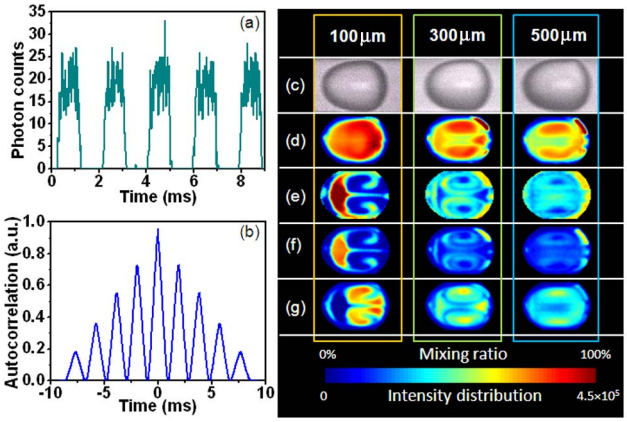

Fig. 3. (Color online) Methods and results of quantitative mapping of two fluid mixing in droplets. (a) Representative line scanning signal of five droplets. (b) Autocorrelation function of corresponding line-scanning signal. (c) Images of droplets taken by a CCD at the locations of 100, 300, and 500 μm from the cross junction. (d) Reconstructed fluorescence intensity images of droplets at corresponding locations. (e) Mixing ratio images of droplets. (f), (g) Fluorescence intensity images for Alexa 430 and Lucifer Yellow dyes.

set by the commercial TCSPC system, each data file could record the line-scanning signals of up to 22 droplets. We first summed up the signals of the droplets recorded in one data file. The summed-up signals from a few data files were then added up into a single signal of much higher counts.

This two-step summing-up process requires precise alignment of the line-scanning signal of each droplet. A time autocorrelation function of the multiple droplet signals is shown in Fig. 3(b). The results demonstrate that droplets were generated accurate periodically. The period calculated from the autocorrelation function was used to divide the signal sequences in a data file and align the signal of each droplet for summing up. In the second step, the summed up signals of different data files were precisely aligned based on their cross-correlation for further summing up.

In this study, we summed up the signals of ~2000 droplets to form a single line-scanning signal and used 43 scanning lines across the channel to form the cross-sectional image of the identical droplets. Complete collection of data for each cross-sectional image requires $2000\,(\text{droplets/line}) \times 43\,(\text{lines})/500\,(\text{droplets/s}) = 172\,\text{s}$. The scanning lines across the channel were aligned by matching the droplet profiles captured by a CCD camera as shown in Fig. 3(c) [7]. To demonstrate the typical mixing patterns, we imaged droplets located at 100, 300, and 500 μm from the droplet forming cross junction. A detailed evolution of mixing dynamics can be obtained from more images at various locations. The fluorescence intensity images are shown in Fig. 3(d). We applied the nonfitting division ratio method to map the mixing ratios of two dye solutions in the droplets. The mixing ratios were calculated from the division ratio by utilizing the calibration curve in Fig. 2(c). The reconstructed mixing ratio images of the Alexa dye are displayed in Fig. 3(e). The results were consistent with the theoretical analyses of the mixing mechanism that two symmetric circulations are generated within droplets that move through a straight channel [11]. To understand the mixing dynamics in the droplets, we extracted the distributions of the Alexa and Lucifer dyes in the droplets. The fluorescence intensity of the Alexa dye at each pixel of the droplet images can be extracted as follows:

$$I_{\text{Alexa}} = \frac{I_{\text{Total}} \times M_{\text{Alexa}} \times F}{M_{\text{Alexa}} \times F + (1 - M_{\text{Alexa}})}, \tag{2}$$

where I_{Total} is the total fluorescence signal and F is a ratio of the fluorescence intensity of pure Alexa solution over pure Lucifer solution measured under the same conditions. The fluorescence intensity of Lucifer was calculated as $I_{\text{Lucifer}} = I_{\text{Total}} - I_{\text{Alexa}}$. The Alexa and Lucifer fluorescence images of the droplets are displayed in Figs. 3(f) and 3(g), respectively. For a fair comparison of signals from two solutions in a droplet, the Lucifer fluorescence intensity signal was normalized to the Alexa signal by multiplying a factor F.

In summary, we studied the mixing dynamics inside microfluidic system generated droplets using two-photon fluorescence lifetime imaging. The mixing patterns of two solutions in the droplets were quantitatively and accurately measured. The technique for characterizing the mixing dynamics of a droplet microfluidic device will positively impact the study of the biological and chemical reaction kinetics in microfluidic systems.

[†]These authors contributed equally to this Letter.

References

1. A. J. de Mello, Nature **442**, 394 (2006).
2. S. Teh, R. Lin, L. Hung, and A. P. Lee, Lab Chip **8**, 198 (2008).
3. D. L. Chen, C. J. Gerdts, and R. F. Ismagilov, J. Am. Chem. Soc. **127**, 9672 (2005).
4. B. K. H. Yen, A. Gunther, M. A. Schmidt, K. F. Jensen, and M. G. Bawendi, Angew. Chem. Int. Ed. **44**, 5447 (2005).
5. T. Robinson, P. Valluri, H. B. Manning, D. M. Owen, I. Munro, C. B. Talbot, C. Dunsby, J. F. Eccleston, G. S. Baldwin, M. A. A. Neil, A. J. de Mello, and P. M. W. French, Opt. Lett. **33**, 1887 (2008).
6. M. Srisa-Art, A. J. de Mello, and J. B. Edel, Phys. Rev. Lett. **101**, 014502 (2008).
7. X. C. I. Solvas, M. Srisa-Art, A. J. de Mello, and J. B. Edel, Anal. Chem. **82**, 3950 (2010).
8. D. Li, W. Zheng, and J. Y. Qu, Opt. Lett. **33**, 2365 (2008).
9. J. T. Coleman, J. McKechnie, and D. Sinton, Lab Chip **6**, 1033 (2006).
10. M. Maus, M. Cotlet, J. Hofkens, T. Gensch, F. C. De Schryver, J. Schaffer, and C. A. M. Seidel, Anal. Chem. **73**, 2078 (2001).
11. W. Tanthapanichakoon, N. Aoki, K. Matsuyama, and K. Mae, Chem. Eng. Sci. **61**, 4220 (2006).